

PLANNING IMMEDIATE LANDMARKS OF TARGETS FOR MODEL-FREE SKILL TRANSFER ACROSS AGENTS

Minghuan Liu¹ Zhengbang Zhu¹ Menghui Zhu¹ Yuzheng Zhuang² Weinan Zhang¹ Jianye Hao²

¹ Shanghai Jiao Tong University, ² Huawei Noah's Ark Lab

{minghuanliu, zhengbangzhu, mhzhu, wnzhang}@sjtu.edu.cn,

{zhuangyuzheng, haojianye}@sjtu.edu.cn

ABSTRACT

In reinforcement learning applications like robotics, agents usually need to deal with various input/output features when specified with different state/action spaces by their developers or physical restrictions. This indicates unnecessary re-training from scratch and considerable sample inefficiency, especially when agents follow similar solution steps to achieve tasks. In this paper, we aim to transfer similar high-level goal-transition knowledge to alleviate the challenge. Specifically, we propose PILOT, i.e., Planning Immediate Landmarks of Targets. PILOT utilizes the universal decoupled policy optimization to learn a goal-conditioned state planner; then, distills a goal-planner to plan immediate landmarks in a model-free style that can be shared among different agents. In our experiments, we show the power of PILOT on various transferring challenges, including few-shot transferring across action spaces and dynamics, from low-dimensional vector states to image inputs, from simple robot to complicated morphology; and we also illustrate a zero-shot transfer solution from a simple 2D navigation task to the harder Ant-Maze task.

1 INTRODUCTION

Reinforcement Learning (RL) has promoted considerable developments in resolving kinds of decision-making challenges, such as games (Yang et al., 2022), robotics (Gu et al., 2017) and even autonomous driving (Zhou et al., 2020). However, those applications only solve a single task with a particular agent state/action space design. When different agents follow similar solution steps to achieve tasks, this will cause unnecessary re-training from scratch and considerable sample inefficiency. This is different from existing transferring tasks, e.g., Transfer RL (Zhu et al., 2020), Meta RL (Wang et al., 2016) or success feature methods (Barreto et al., 2017) aim to dynamics/reward with the same agent, instead of the shared knowledge across agents with different state/action spaces.

In this paper, we consider transferring similar high-level goal-transition knowledge to help different agents learn better. For example, different robots can share a global positioning system constructed by techniques like GPS or SLAM

that allows them to quickly figure out their 2D/3D positions in the world, and thus can share the navigation knowledge to help them quickly finish their tasks. Besides, such transferring solution also benefits us from: a) deployed agents facing changed observing features, for instance, non-player characters (NPC) trained and updated for incremental scenes of games (Juliani et al., 2018), robots with new sensors due to hardware replacement (Bohez et al., 2017); b) agents in different

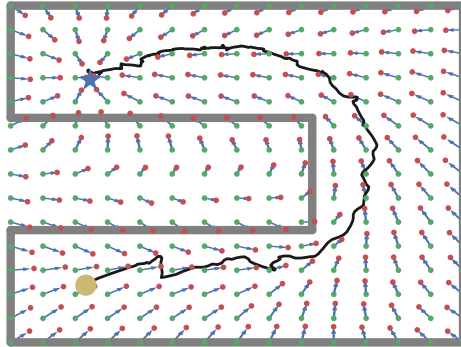


Figure 1: Zero-shot transferring on *Ant-Maze*, where the Ant agent starts from the big green point and samples a trajectory (black line) to the desired goal (big blue star). PILOT provides planned immediate landmarks (small red points) given the current goal state (small green points) and the desired goal (blue star), learned from a naive 2D maze task. Note that points outside the maze are also provided for prediction to show the property of the planned goals matches the appearance of the maze.

morphology have to finish the same tasks (Gupta et al., 2021), such as run a complicate quadruped robotic following a much simpler simulated robot (Peng et al., 2018); c) improving the learning efficiency with rich and redundant observations or complicate action spaces, like transferring the knowledge from compact low-dimensional vector input to high-dimensional image features (Sun et al., 2022).

In this paper, we propose a general solution for transferring multi-task skills across agents with heterogeneous action spaces and observation spaces, named Planning Immediate Landmarks of Targets (PILoT). Our method works under the assumption that agents share the same goal transition to finish tasks, but without any prior knowledge of the inter-task mapping between the different state/action spaces, and agents can not interact with each other.

The whole workflow of PILoT is composed of three stages, including pre-training, distillation and transfer: 1) the *pre-training stage* extends the decoupled policy to train a universal state planner on simple tasks with universal decoupled policy optimization; 2) the *distillation stage* distills the knowledge of state planner into an immediate goal planner, which is then utilized to 3) the *transferring stage* that plans immediate landmarks in a model-free style serving as dense rewards to improve the learning efficiency or even straightforward goal guidance. Fig. 1 provides a quick overview of our algorithm for zero-shot transferring on Ant-Maze. Correspondingly, we first train a decoupled policy on a simple 2D maze task to obtain a universal state planner, then distill the knowledge into a goal planner that predicts the immediate target goal (red points) to reach given the desired goal (blue point) and arbitrary started goal (green points). Following the guidance, the Ant controllable policy is pre-trained on free ground without the walls and can be directly deployed in the maze environment without any training. As the name suggests, we are providing immediate landmarks to guide various agents like the runway center line light on the airport guiding the flight to take off.

Comprehensive challenges are designed to examine the superiority of PILoT on the skill transfer ability, we design a set of hard transferring challenges, including few-shot transfer through different action spaces and action dynamics, from low-dimensional vectors to image inputs, from simple robots to complicated morphology, and even zero-shot transfer. The experimental results present the learning efficiency of PILoT transferred on every task by outperforming various baseline methods.

2 PRELIMINARIES

Goal-Augmented Markov Decision Process. We consider the problem of goal-conditioned reinforcement learning (GCRL) as a γ -discounted infinite horizon goal-augmented Markov decision process (GA-MDP) $\mathcal{M} = \langle \mathcal{S}, \mathcal{A}, \mathcal{T}, \rho_0, r, \gamma, \mathcal{G}, p_g, \phi \rangle$, where \mathcal{S} is the set of states, \mathcal{A} is the action space, $\mathcal{T} : \mathcal{S} \times \mathcal{A}^k \rightarrow \mathcal{S}$ is the k -step environment dynamics function (in this paper we only work on deterministic environment dynamics so \mathcal{T} gives a deterministic output given a specific state and action sequence), $\rho_0 : \mathcal{S} \rightarrow [0, 1]$ is the initial state distribution, and $\gamma \in [0, 1]$ is the discount factor. The agent makes decisions through a policy $\pi(a|s) : \mathcal{S} \rightarrow \mathcal{A}$ and receives rewards $r : \mathcal{S} \times \mathcal{A} \rightarrow \mathbb{R}$, in order to maximize its accumulated reward $R = \sum_{t=0}^{\infty} \gamma^t r(s_t, a_t)$. Additionally, \mathcal{G} denotes the goal space w.r.t tasks, p_g represents the desired goal distribution of the environment, and $\phi : \mathcal{S} \rightarrow \mathcal{G}$ is a tractable mapping function that maps the state to a specific goal. One typical challenge in GCRL is reward sparsity, where usually the agent can only be rewarded once it reaches the goal:

$$r_g(s_t, a_t, g) = \mathbb{1}(\text{the goal is reached}) = \mathbb{1}(\|\phi(s_{t+1}) - g\| \leq \epsilon). \quad (1)$$

Therefore, GCRL focuses on multi-task learning where the task variation comes only from the difference of the reward function under the same dynamics. To shape a dense reward, a straightforward idea is to utilize a distance measure d between the achieved goal and the final desired goal, *i.e.*, $\tilde{r}_g(s_t, a_t, g) = -d(\phi(s_{t+1}), g)$. However, this reshaped reward will fail when the agent must first increase the distance to the goal before finally reaching it, especially when there are obstacles on the way to the target (Trott et al., 2019).

Decoupled Policy Optimization Classical RL methods learn a state-to-action mapping policy function, whose optimality is ad-hoc to a specific task. In order to free the agent to learn a high-level planning strategy that can be used for transfer, Liu et al. (2022b) proposed Decoupled Policy Optimization (DePO) which decoupled the policy structure by a state transition planner h and an

inverse dynamics model I as:

$$\pi(\cdot|s) = \int_{s'} h_\pi(s'|s) I(\cdot|s, s') ds' = \mathbb{E}_{s' \sim h_\pi(s'|s)} [I(\cdot|s, s')]. \quad (2)$$

To optimize the decoupled policy, DePO first optimizes the inverse dynamics model via supervised learning, and then performs policy gradient assuming a fixed but locally accurate inverse dynamics function. DePO provides a way of planning without training an environment dynamics model. The state planner of DePO pre-trained on simple tasks can be further transferred to agents with various action spaces or dynamics. However, as noted below, the transferring ability of DePO limits in the same state space transition. In this paper, we aim to derive a more generalized skill-transferring solution utilizing the common latent goal space shared among tasks and agents.

3 TRANSFER ACROSS AGENTS

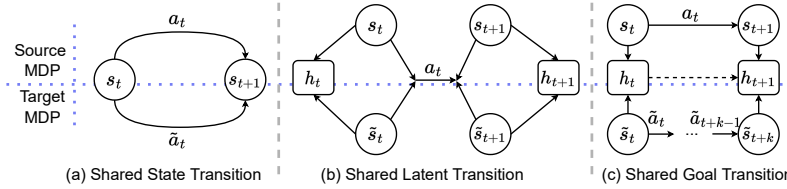


Figure 2: Comparison of the different assumptions for transferring across agents of previous works (Liu et al., 2022b; Sun et al., 2022) and PILoT. (a) (Liu et al., 2022b) allows for transferring across action spaces but asks for the same state space and state transition. (b) (Sun et al., 2022) transfers across different state spaces but requires there exists a shared latent state space and dynamics. (c) PILoT provides a generalized transferring ability for both state space and action space, but asks for a shared underlying latent goal transition.

In this section, we explain the problem setup of transfer across agents. Formally, we pre-train and learn knowledge from a source GA-MDP $\mathcal{M} = \langle \mathcal{S}, \mathcal{A}, \mathcal{T}, \rho_0, r, \gamma, \mathcal{G}, p_g, \phi \rangle$ and transfer to a target GA-MDP $\tilde{\mathcal{M}} = \langle \tilde{\mathcal{S}}, \tilde{\mathcal{A}}, \tilde{\mathcal{T}}, \tilde{\rho}_0, \tilde{r}, \tilde{\gamma}, \tilde{\mathcal{G}}, \tilde{p}_g, \tilde{\phi} \rangle$. Here we allow significant differences between the state spaces $\mathcal{S}, \tilde{\mathcal{S}}$, and action spaces $\mathcal{A}, \tilde{\mathcal{A}}$. Therefore, both the input/output shapes of the source policy are totally different from the target one and therefore it is challenging to transfer shared knowledge.

To accomplish the objective of transfer across agents, prior works made assumptions about the shared structure (Fig. 2). For example, (Sun et al., 2022) proposed to transfer across significantly different state spaces with the same action space and similar structure between dynamics, *i.e.*, a mapping between the source and target state spaces exists such that the transition dynamics shares between two tasks under the mapping. In comparison, (Liu et al., 2022b) paid attention to transferring across action spaces under the same state space and state transitions, *i.e.*, an action mapping between the source and target exists such that the transition dynamics shares between two tasks under the mapping. In this paper, instead of restricting the same state/action spaces, we take a more general assumption by only requiring agents have a shared goal transition, and allow transferring across different observation spaces and action spaces. Formally, the assumption corresponds to:

Assumption 1. *There exists an k -step action sequence $A^k = \{a_t, \dots, a_{t+k}\}$ such that $\forall s, s' \in \mathcal{S}, \forall a \in \mathcal{A}$, and $\exists \tilde{s}, \tilde{s}' \in \tilde{\mathcal{S}}$,*

$$\mathcal{T}(s'|s, a) = \tilde{\mathcal{T}}(\tilde{s}'|\tilde{s}, A^k), r(s, a, g^t) = \tilde{r}(\tilde{s}, \tilde{a}, g^t), \phi(s) = \tilde{\phi}(\tilde{s}), \phi(s') = \tilde{\phi}(\tilde{s}').$$

Here ϕ is usually a many-to-one mapping, such as an achieved position or the velocity of a robot. f can be any function, like many-to-one mapping, where several target actions relate to the same source action; or one-to-many mapping; or non-surjective, where there exists a source action that does not correspond to any target action.

4 PLANNING IMMEDIATE LANDMARKS OF TARGETS

In this section, we introduce our generalized multi-task skills transfer solution with the proposed Planning Immediate Landmarks of Targets (PILoT) framework. First, we demonstrate how we derive the training procedure of a universal decoupled policy structure for multiple tasks in the

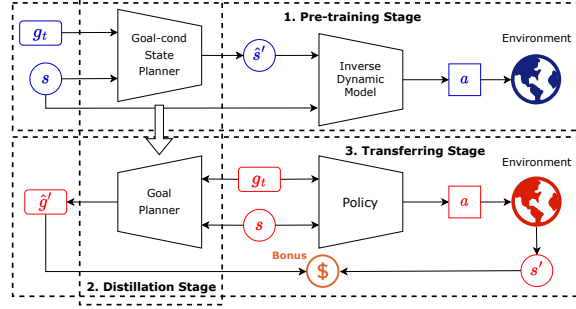


Figure 3: Overview of a general transferring usage of Planning Immediate Landmarks of Target (PILoT) framework, including (1) pre-training, (2) distillation, and (3) transferring stages, where we use different colors to denote different (*state/goal/action*) spaces. (1) The pre-training stage trains a decoupled policy on a source agent and learn a goal-conditioned state planner (Section 4.1); (2) The distillation stage distills the state planner into a goal planner (Section 4.2); (3) The transferring stage transfers the knowledge in different ways (Section 4.3). Note that other than utilizing the reward bonus in transfer learning the target agent, the state planner can also be directly transferred into another decoupled policy, and the goal planner can be used for providing immediate targets for pre-trained controllers.

pre-training stage, which is used for obtaining a goal planner in the distillation stage (Section 4.2); the distilled goal planner is further used for providing the informative reward bonus or zero-shot guidance for the transferring stage (Section 4.3). An overview of the method is shown in Fig. 3, and we list the step-by-step algorithm in Algo. 1.

4.1 UNIVERSAL DECOUPLED POLICY OPTIMIZATION

In order to derive a generally transferable solution, we extend the decoupled policy structure (Liu et al., 2022b) into a goal-conditioned form. Formally, we decouple the goal-conditioned policy $\pi(a|s, g^t)$ as:

$$\pi(a|s, g^t) = \int_{s'} h_\pi(s'|s, g^t) I(\cdot|s, s') ds' = \mathbb{E}_{\hat{s}' \sim h_\pi(\hat{s}'|s, g^t)} [I(\cdot|s, \hat{s}')], \quad (3)$$

where g^t is the target goal, h_π is a goal-conditioned state planner. Approximating the planner by neural networks (NNs), we can further apply the reparameterization trick and bypass explicitly computing the integral over s' as

$$s' = h(\epsilon; s, g^t), \quad \pi(a|s, g^t) = \mathbb{E}_{\epsilon \sim \mathcal{N}} [I(a|s, h(\epsilon; s, g^t))], \quad (4)$$

where ϵ is an input noise vector sampled from some fixed distribution, like a Gaussian. The inverse dynamics I should serve as a control module known in advance for reaching the target predicted by the planner. When it must be learned from scratch, we can choose to minimize the divergence (for example, KL) between the inverse dynamics of a sampling policy $\pi_{\mathcal{B}}$ (buffer samples) and the ϕ -parameterized function I_ϕ , i.e.,

$$\min_{\psi} L^I = \mathbb{E}_{(s, s') \sim \pi_{\mathcal{B}}} [\mathbf{D}_f(I_{\pi_{\mathcal{B}}}(a|s, s') \| I_\phi(a|s, s'))]. \quad (5)$$

It is worth noting that the model is only responsible and accurate for states encountered by the current policy instead of the overall state space. As a result, the inverse dynamics model is updated every time before updating the policy.

To update the decoupled policy, particularly, the goal-conditioned state planner h_π , given that the inverse dynamics is an accurate local control module for the current policy and the inverse dynamics function I is static when optimizing the policy function, we adopt the decoupled policy gradient (DePG) as derived in Liu et al. (2022b):

$$\nabla_{\psi} \mathcal{L}^{\pi} = \mathbb{E}_{(s, a) \sim \pi, g^t \sim p_g, \epsilon \sim \mathcal{N}} \left[\frac{Q(s, a, g)}{\pi(a|s, g^t)} (\nabla_h I(a|s, h_{\psi}(\epsilon; s, g^t)) \nabla_{\psi} h_{\psi}(\epsilon; s, g^t)) \right], \quad (6)$$

which can be seen as taking the knowledge of the inverse dynamics about the action a to optimize the planner by a prediction error $\Delta s' = \alpha \nabla_h I(a|s, h(\epsilon; s))$ where α is the learning rate. However, Liu et al. (2022b) pointed out that there exists an agnostic gradient problem. Particularly, the gradient for updating the state planner may lead to arbitrary illegal states that can obtain desired actions that

maximize the return through inverse dynamics (represented by NNs). To alleviate this, they proposed calibrated decoupled policy gradient to ensure the state planner from predicting an infeasible state transition. In this paper, we turn to a simpler additional objective for constraints, *i.e.*, we maximize the probability of predicting the legal transitions that are sampled by the current policy, which still retains good performance in Liu et al. (2022b):

$$\max \mathbb{E}_{(s,s') \sim \pi} [h(s'|s, g^t)], \quad (7)$$

Therefore, the final gradient for updating the planner becomes:

$$\nabla_{\psi} \mathcal{L}^{\pi} = \mathbb{E}_{(s,a,s') \sim \pi, g^t \sim p_g, \epsilon \sim \mathcal{N}} \left[\frac{Q(s,a,g)}{\pi(a|s,g^t)} (\nabla_{hI}(a|s, h_{\psi}(\epsilon; s, g^t)) \nabla_{\psi} h_{\psi}(\epsilon; s, g^t)) + \lambda \nabla_{\psi} h_{\psi}(\epsilon; s, g^t) \right], \quad (8)$$

where λ is the hyperparameter for trading off the constraint. Learn goal-conditioned policies with decoupled optimization, we can also incorporate various relabeling strategies to further improve the sample efficiency, as in HER (Andrychowicz et al., 2017), *i.e.*, we relabel every transition when we draw them out from the replay buffer to train our policy.

4.2 GOAL PLANNER DISTILLATION

In order to transfer the knowledge to new settings, we leverage the shared latent goal space and distill a goal planner from the goal-conditioned state planner, *i.e.*, we want to predict the consecutive goal given the current goal and the target goal. Formally, we aim to obtain a ω -parameterized function $f_{\omega}(g'|g, g^t)$, where g' is the next goal to achieve, $g = \phi(s)$ is the current goal the agent is achieved, and g^t is the target. This can be achieved by treating the state planner $h_{\psi}(s'|s, g^t)$ as the teacher, and $f_{\omega}(g'|g, g^t)$ becomes the student. The objective of the distillation is constructed as an MLE loss:

$$\nabla_{\omega} \mathcal{L}^f = \max_{\omega} \mathbb{E}_{s \sim \mathcal{B}, \tilde{s}' \sim h_{\psi}, g^t \sim p_g} [f_{\omega}(\tilde{g}'|g, g^t)], \text{ where } g = \phi(s), \tilde{g}' = \phi(\tilde{s}'), \quad (9)$$

where \mathcal{B} is the replay buffer, ϕ is the mapping function that translates a state to a specific goal. With the distilled goal planner, we can now conduct goal planning without training and querying an environment dynamics model as in Zhu et al. (2021); Chua et al. (2018).

4.3 TRANSFER MULTI-TASK KNOWLEDGE ACROSS AGENTS

A typical challenge for GCRL is the rather sparse reward function, and simply utilizing the Euclidean distance of the final goal and the current achieved goal can lead to additional sub-optimal problems. To this end, with PILoT having been distilled for acquiring plannable goal transitions, it is natural and general to construct a reward function (or bonus) leveraging the difference between the intermediate goals to reach and the goal that actually achieves for transfer learning a new policy. In particular, when the agent aims to go to g_t with the current achieved goal g , we exploit the distilled planner f_{ω} from PILoT to provide rewards as similarity of goals:

$$r(s, a, \hat{g}') = \frac{\phi(s') \cdot \hat{g}'}{\|\phi(s')\| \|\hat{g}'\|}, \text{ where } s' = \mathcal{T}(s, a), \hat{g}' \sim f_{\omega}(\hat{g}'|g, g^t). \quad (10)$$

Note that we avoid the different scale problems among different agents by using the form of cosine distance. Thereafter, we can actually transfer to a totally different agent. For example, we can learn a locomotion task from an easily controllable robot, and then transfer the knowledge to a complex one with more joints which is hard to learn directly from the sparse rewards; or we can learn from a low-dimensional ram-based agent and then transfer on high-dimensional image inputs. Other than transferring over rewards, when the action space and action dynamics of the target agents are the same as the source agent, we can transfer the decoupled policy where the goal-conditioned state planner can be directly used for the target agents without any further training, and only the inverse dynamics model should be re-trained; besides, the distilled goal planner also supports zero-shot transferring on pre-trained controllers by providing immediate goals along every step.

5 RELATED WORK

Goal-conditioned RL. Our work lies in the formulation of goal-conditioned reinforcement learning (GCRL), which aims to learn a generalized policy and settle a group of homogeneous tasks with

different goals simultaneously. The existence of goals, which can be explained as skills, tasks, or targets, makes it possible for our skill transfer across various agents with different state/action space. In the literature of GCRL, researchers focus on alleviating the challenges in learning efficiency and generalization ability, from the perspective of optimization [Trott et al. \(2019\)](#); [Ghosh et al. \(2021\)](#); [Zhu et al. \(2021\)](#), generating or selecting sub-goals [Florensa et al. \(2018\)](#); [Pitis et al. \(2020\)](#) and relabeling [Andrychowicz et al. \(2017\)](#); [Zhu et al. \(2021\)](#). A comprehensive GCRL survey can be further referred to [Liu et al. \(2022a\)](#). In these works, the goal given to the policy function is either provided by the environment or proposed by a learned function. In comparison, in our paper, the proposed UDPO algorithm learns the next target states in an end-to-end manner which can be further distilled into a goal planner that can be used to propose the next target goals.

Hierarchical reinforcement learning. The framework of UDPO resembles Hierarchical Reinforcement Learning (HRL) structures, where the state planner plays like a high-level policy and the inverse dynamics as the low-level policy. A typical paradigm of HRL trains the high-level policy using environment rewards to predict sub-goals (or called options) that the low-level policy should achieve, and learn the low-level policy using handcrafted goal-reaching rewards to provide the action and interacts with the environment. Generally, most of works provided the sub-goals / options by the high-level policy are lied in a learned latent space ([Konidaris & Barto, 2007](#); [Heess et al., 2016](#); [Kulkarni et al., 2016](#); [Vezhnevets et al., 2017](#); [Zhang et al., 2022](#)), keeping it for a fixed timesteps ([Nachum et al., 2018](#); [Vezhnevets et al., 2017](#)) or learn to change the option ([Zhang & Whiteson, 2019](#); [Bacon et al., 2017](#)). On the contrary, [Nachum et al. \(2018\)](#) and [Kim et al. \(2021\)](#) both predicted sub-goals in the raw form, while training the high-level and low-level policies with separate objectives. As for [Nachum et al. \(2018\)](#), they trained the high-level policy in an off-policy manner; and for [Kim et al. \(2021\)](#), which focused on goal-conditioned HRL tasks as ours, they sampled and selected specific landmarks according to some principles, and asked the high-level policy to learn to predict those landmarks. Furthermore, they only sampled a goal from the high-level policy for fixed steps, otherwise using a pre-defined goal transition process. Like UDPO, [Li et al. \(2020\)](#) optimized the two-level hierarchical policy in an end-to-end way, with a latent skill fixed for c timesteps. The main contribution of HRL works concentrates on improving the learning efficiency on complicated tasks, yet UDPO aims to obtain every next target for efficient transfer.

Transferable RL. Before our work, a few works have investigated transferable RL. In this endeavor, [Srinivas et al. \(2018\)](#) proposed to transfer a visual encoder learned in source tasks, which is further used for computing the latent distance from the goal image to the current observation and is used to construct an obstacles-aware reward function in target tasks/agents. To transfer across tasks, [Barreto et al. \(2017\)](#); [Borsa et al. \(2018\)](#) utilized success features based on strong assumptions about the reward formulation, that decouples the information about the dynamics and the rewards into separate components, so that only the relevant module needs to be retrained when the task changes. In order to reuse the policy, [Heess et al. \(2016\)](#) learned a bi-level policy structure, composed of a low-level domain-general controller and a high-level task-specific controller. They transfer the low-level controller to the target tasks while retraining the high-level one. On the other hand, [Liu et al. \(2022b\)](#) decoupled the policy as a state planner and an inverse dynamic model, and showed the state planner can be transferred to agents with different action spaces. For generalizing and transferring across modular robots’ morphology, [Gupta et al. \(2017\)](#) tried learning invariant visual features. Some works exploited graph structure present in the agent’s morphology, and [Wang et al. \(2018\)](#) and [Huang et al. \(2020\)](#) both proposed specific structured policies for learning the correlations between the agent’s components, while [Gupta et al. \(2021\)](#) and [Kurin et al. \(2020\)](#) proposed transformer-based policies to model the morphology representation. These works with such structured policies, although can generalize to agents with unseen morphology, limit in modular robots with pre-designed representation form of the state space. [Sun et al. \(2022\)](#) proposed to transfer across agents with different state spaces, which is done with a latent dynamics model trained on the source task. On the target tasks, the pre-trained dynamics model is transferred as a model-based regularizer for improving learning efficiency. Different from these methods, PILoT effectively transfers multi-task skills to agents with different structures, state/action spaces in a model-free style. First, the decoupled policy structure separates the state spaces and action spaces, allowing the state predictor directly be transferred to agents with different action spaces. Furthermore, the distilled goal planner can be transferred to agents with different structures and state spaces by planning immediate sub-goals.

6 EXPERIMENTS

We conduct a set of transferring challenges to examine how we can use PILoT for transfer.

6.1 EXPERIMENTAL SETUPS

Environments, tasks and agents. a) *Fetch-Reach*. The agent controls the robot arm to reach a target position. b) *Fetch-Push*. The robotic arm is controlled to push a block to a target position. c) *Reacher*. Controlling a multi-joint reacher robot to reach a target position. d) *Point-Locomotion*. The agent controls a point robot to move to a target position freely. e) *Ant-Locomotion*. The agent controls an ant robot to move to a target position freely. f) *2D-Maze*. The agent controls a mass point in a U-shape maze to reach a target position. g) *Ant-Maze*. The agent controls an ant robot to move to a target position in a U-shape maze.

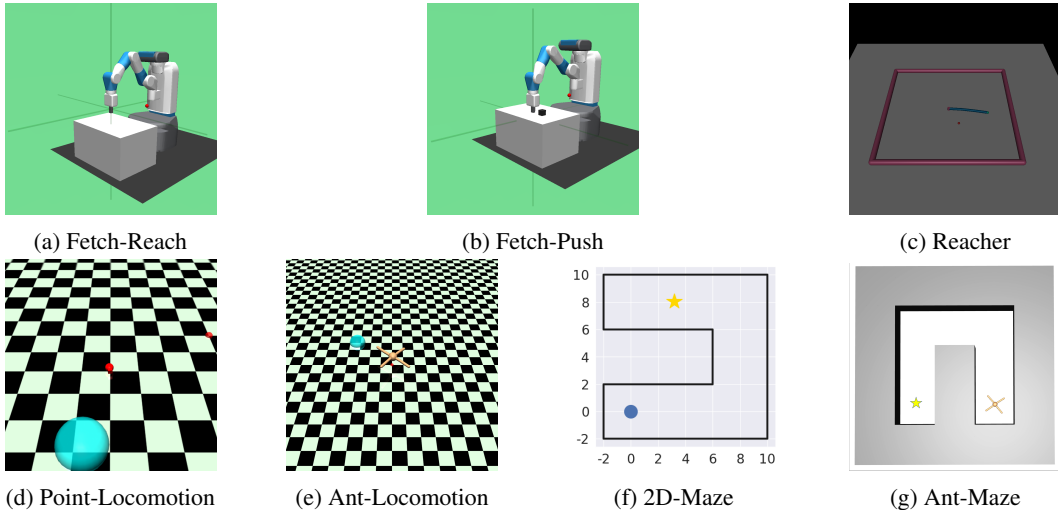


Figure 4: Illustration of tested environments.

Designed transferring challenges. 1) **Few-shot transfer to high-dimensional action spaces:** we take *Fetch-Reach* and *Fetch-Push* as the source tasks, and change the gravity, action dynamics and spaces to get the target tasks while sharing the same state space and state transition (see Appendix B.2 for details). 2) **Few-shot transfer to a complicated morphology:** we take *Point* robot with 6 observation dimensions as the source task, and *Ant* with 29 observation dimensions as the target task. 3) **Few-shot transfer from vector to image observations:** we take *Fetch-Reach* and *Reacher* with low-dimensional vector state as the source task, and the same environment with high-dimensional image observations as the target task. 4) **Zero-shot transfer:** we take *2D-Maze* (for training a goal planner) and *Ant-Locomotion* (for training a uniform controller/policy) as the source tasks; then we combine the knowledge of the goal planner and the uniform controller to master the task of *Ant-Maze* without any further training. All of these tasks varies in either the state space or the action space, but a pair of tasks must share the same goal space and transition, making it possible to transfer useful knowledge. In the sequel, we show different usages of PILoT on transferring such knowledge in different challenges.

Implementation and baselines. We choose several classical and recent representative works as our comparable baselines, for both source tasks and target tasks. For source tasks we want to compare the learning performance from scratch of the proposed UDPO algorithm with: i) **Hindsight Experience Replay (HER)** (Andrychowicz et al., 2017), a classical GCRL algorithm that trains goal-conditioned policy by relabeling the target goals as the samples appeared in future of the same trajectory for one particular state-action training sample, which is also used as the basic strategy to train the UDPO policy; ii) **Hierarchical reinforcement learning Guided by Landmarks (HIGL)** (Kim et al., 2021), an HRL algorithm that is structure-similar to UDPO by utilizing a high-level policy

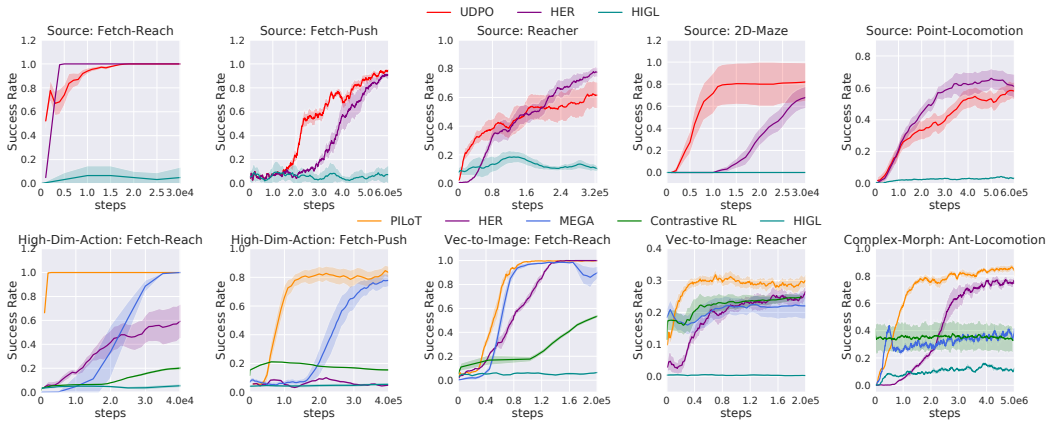


Figure 5: Training curves on five source tasks and five target tasks. High-Dim-Action: few-shot transfer to high-dimensional action space. High-Dim-Action: few-shot transferring to high-dimensional action space. Vec-to-Image: few-shot transferring from vector to image states. Complex-Morph: few-shot transfer to different morphology. UDPO denotes the learning algorithm proposed in Section 4.1.

to propose landmark states for the low-level policy to explore. As for the target tasks, we aim to show the transferring ability of PILoT from source tasks to target tasks, except HER and HIGL, we also compare a recent well-performed GCRL algorithm, **Maximum Entropy Gain Exploration (MEGA)** (Pitis et al., 2020), which proposed to enhance the exploration coverage of the goal space by sampling goals that maximize the entropy of past achieved goals; also, a very recent algorithm, **Contrastive RL** (Eysenbach et al., 2022), which design a contrastive representation learning solution for GCRL. These baselines are chosen since they are expected to have great learnability on goal-conditioned tasks. Noted that contrastive RL requires the goal space the same as the state space (e.g., both are images). For each baseline algorithm, we either take their suggested hyperparameters, or try our best to tune important ones.

In our transferring experiments, we first trains the decoupled policy by UDPO with HER’s relabeling strategy for all source tasks; then, the state planner can be transferred into a decoupled policy structure directly (High-Dim-Action challenge); or distill the goal planner that can (i) generate dense reward signals to train a normal policy by HER in the target tasks (general challenges), or (ii) providing immediate sub-goals for pre-trained controllers (zero-shot transferring).

6.2 RESULTS AND ANALYSIS

In the main context, we focus on presenting the training results on source tasks and the transferring results on target tasks. Additionally, we leave in-depth analysis, ablation studies and hyperparameter choices in the Appendix C.

Learning in the source tasks. We first train UDPO on five source tasks, and show the training curve in Fig. 5. Note that we do not expect UDPO to be better than HER which learn a normal policy. But from Fig. 5, we observe that UDPO achieves compatible performance, and sometimes it shows better efficiency. Due to the structure similarity of UDPO and HRL methods, we also include a HRL baseline – HIGL on these source tasks. To our surprise, HIGL performs badly or even fails in many tasks, indicating its sensitivity by its landmarks sampling strategy. In Appendix C.1 we further illustrate the MSE error between the planned state and the real state that the agent actually achieved, with the visualization of the planning states, demonstrating that UDPO has a great planning ability under goal-conditioned challenges.

Few-shot transferring to high-dimensional action spaces. The High-Dim-Action transferring challenge requires the agent to generalize its state planner to various action spaces and action dynamics. In our design, the target task has higher action dimension with different dynamics (see Appendix B.2 for details), making the task hard to learn from scratch. As shown in Fig. 5, on the target *Fetch-Rich* and *Fetch-Push*, HER is much more struggle to learn well as it is in the source tasks, and all GCRL, HRL and contrastive RL baselines can only learn with much more samples or even fail. For PILoT, since the source and the target tasks share the same state space and state

transition, we can transfer the goal-conditioned state planner to a new decoupled policy which only have to train the inverse dynamics from scratch. In a result, PILoT shows an incredible efficiency advantage for transferring the shared knowledge to new tasks.

Few-shot transfer from vector to image states. The `Vec-to-Image` transferring challenge learns high-dimensional visual observation input-based policy from scratch guided by the planned goals learned from the low-level vector input. Note that we do not use any pre-training embeddings for visual inputs. Fig. 5 indicates that by simply augmenting HER with additional transferring reward, PILoT achieves the best learning efficiency and final performance on the two given tasks, compared with various baselines that are designed with complicated techniques.

Few-shot transferring to different morphology. We further test the `Complex-Morph` transferring challenge that requires distilling the locomotion knowledge from a simple Point robot to a much more complex Ant robot. Fig. 5 again show the impressive transferring performance of PILoT, while we surprisingly find that MEGA, HIGL and contrastive RL all can hardly learn feasible solutions on this task, even worse than HER. In our further comparison, we find that this tested task is actually more hard to determine the success by requiring the agent to reach at a very close distance (*i.e.*, less than 0.1, which can be further referred to Appendix B). In addition, the reason why MEGA fails to reach a good performance like the other tasks can be attributed to its dependency on an exploration strategy, which always chooses rarely achieved goals measured by its lowest density. This helps a lot in exploration when the target goals’ distribution is dense, like *Ant-Maze*. However, when the goals are scattered as in *Ant-Loocomotion*, the agent has to explore a wide range of the goal space, which may lead MEGA’s exploration strategy to be inefficient. In comparison, PILoT shows that, despite the task being difficult or the target goals being hard-explored, as long as we can transfer necessary knowledge from similar source tasks, agents can learn the skills quickly in a few interactions.

Zero-shot transfer for different layouts. Finally, as we find the intermediate goals provided by the goal planner are accurate enough for every step that the agent encounters, we turn to an intuitive and interesting zero-shot knowledge transfer experiment for different map layouts. Specifically, we try to learn the solution on *Ant-Maze*, as shown in Fig. 4, which is a hard-exploring task since the wall between the starting point and the target position requires the agent to first increase the distance to the goal before finally reaching it. As Fig. 6 illustrates, simply deploying HER fails. With sufficient exploration, all recent GCRL, HRL and contrastive RL baselines can learn a feasible solution after a quite large time of sampling. However, PILoT provides a simpler way by distilling the goal transition knowledge from a much simpler *2D-Maze* task, we take the intermediate goals learned in *2D-Maze* as short guidance (as shown in Fig. 1) for the uniform policy pre-trained in the source *Ant-Loocomotion* task which is trained to reach arbitrary goals within the map. In this way, PILoT can accomplish zero-shot transfer performance without any sampling. This shows a promising disentanglement of goal planners and motion controllers for resolving complex tasks.

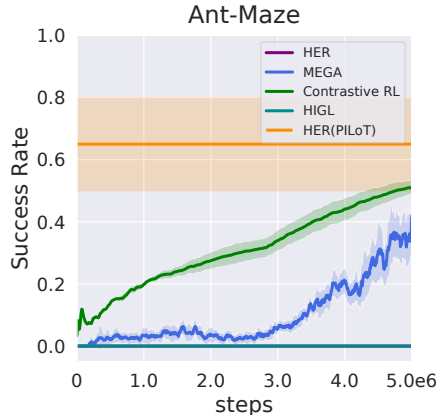


Figure 6: Training and zero-shot transferring curves on *Ant-Maze* task across 10 seeds.

7 CONCLUSION AND LIMITATION

In this paper, we provide a general solution for skill transferring across various agents. In particular, We propose PILoT, *i.e.*, Planning Immediate Landmarks of Targets. First, PILoT utilizes and extends a decoupled policy structure to learn a goal-conditioned state planner by universal decoupled policy optimization; then, a goal planner is distilled to plan immediate landmarks in a model-free style that can be shared among different agents. To validate our proposal, we further design kinds of transferring challenges and show different usages of PILoT, such as few-shot transferring across different action spaces and dynamics, from low-dimensional vector states to image inputs, from simple robot to complicated morphology; we also show a promising case of zero-shot transferring on the harder *Ant-Maze* task. However, we find that the proposed PILoT solution is mainly limited

in those tasks that have clear goal transitions that can be easily distilled, such as navigation tasks; on the contrary, for those tasks which take the positions of objects as goals, it will be much harder to transfer the knowledge since the goals are always static when agents do not touch the objects. We leave those kinds of tasks as future work.

REFERENCES

- Marcin Andrychowicz, Filip Wolski, Alex Ray, Jonas Schneider, Rachel Fong, Peter Welinder, Bob McGrew, Josh Tobin, OpenAI Pieter Abbeel, and Wojciech Zaremba. Hindsight experience replay. In *Advances in Neural Information Processing Systems*, volume 30, 2017.
- Pierre-Luc Bacon, Jean Harb, and Doina Precup. The option-critic architecture. In *Proceedings of the AAAI Conference on Artificial Intelligence*, volume 31, 2017.
- André Barreto, Will Dabney, Rémi Munos, Jonathan J Hunt, Tom Schaul, Hado P van Hasselt, and David Silver. Successor features for transfer in reinforcement learning. *Advances in neural information processing systems*, 30, 2017.
- Steven Bohez, Tim Verbelen, Elias De Coninck, Bert Vankeirsbilck, Pieter Simoens, and Bart Dhoedt. Sensor fusion for robot control through deep reinforcement learning. In *International Conference on Intelligent Robots and Systems*, pp. 2365–2370. Ieee, 2017.
- Diana Borsa, André Barreto, John Quan, Daniel Mankowitz, Rémi Munos, Hado Van Hasselt, David Silver, and Tom Schaul. Universal successor features approximators. *arXiv preprint arXiv:1812.07626*, 2018.
- Kurtland Chua, Roberto Calandra, Rowan McAllister, and Sergey Levine. Deep reinforcement learning in a handful of trials using probabilistic dynamics models. In *Advances in Neural Information Processing Systems*, volume 31, 2018.
- Benjamin Eysenbach, Tianjun Zhang, Ruslan Salakhutdinov, and Sergey Levine. Contrastive learning as goal-conditioned reinforcement learning. *arXiv preprint arXiv:2206.07568*, 2022.
- Carlos Florensa, David Held, Xinyang Geng, and Pieter Abbeel. Automatic goal generation for reinforcement learning agents. In *International Conference on Machine Learning*, pp. 1515–1528. PMLR, 2018.
- Dibya Ghosh, Abhishek Gupta, Ashwin Reddy, Justin Fu, Coline Devin, Benjamin Eysenbach, and Sergey Levine. Learning to reach goals via iterated supervised learning. *International Conference on Learning Representations*, 2021.
- Shixiang Gu, Ethan Holly, Timothy Lillicrap, and Sergey Levine. Deep reinforcement learning for robotic manipulation with asynchronous off-policy updates. In *International Conference on Robotics and Automation*, pp. 3389–3396. IEEE, 2017.
- Abhishek Gupta, Coline Devin, YuXuan Liu, Pieter Abbeel, and Sergey Levine. Learning invariant feature spaces to transfer skills with reinforcement learning. *arXiv preprint arXiv:1703.02949*, 2017.
- Agrim Gupta, Linxi Fan, Surya Ganguli, and Li Fei-Fei. Metamorph: Learning universal controllers with transformers. In *International Conference on Learning Representations*, 2021.
- Nicolas Heess, Greg Wayne, Yuval Tassa, Timothy Lillicrap, Martin Riedmiller, and David Silver. Learning and transfer of modulated locomotor controllers. *arXiv preprint arXiv:1610.05182*, 2016.
- Wenlong Huang, Igor Mordatch, and Deepak Pathak. One policy to control them all: Shared modular policies for agent-agnostic control. In *International Conference on Machine Learning*, pp. 4455–4464. PMLR, 2020.
- Arthur Juliani, Vincent-Pierre Berges, Ervin Teng, Andrew Cohen, Jonathan Harper, Chris Elion, Chris Goy, Yuan Gao, Hunter Henry, Marwan Mattar, et al. Unity: A general platform for intelligent agents. *arXiv preprint arXiv:1809.02627*, 2018.

- Junsu Kim, Younggyo Seo, and Jinwoo Shin. Landmark-guided subgoal generation in hierarchical reinforcement learning. In *Advances in Neural Information Processing Systems*, volume 34, pp. 28336–28349, 2021.
- George Dimitri Konidaris and Andrew G Barto. Building portable options: Skill transfer in reinforcement learning. In *International Joint Conference on Artificial Intelligence*, volume 7, pp. 895–900, 2007.
- Tejas D Kulkarni, Karthik Narasimhan, Ardavan Saeedi, and Josh Tenenbaum. Hierarchical deep reinforcement learning: Integrating temporal abstraction and intrinsic motivation. *Advances in Neural Information Processing Systems*, 29, 2016.
- Vitaly Kurin, Maximilian Igl, Tim Rocktäschel, Wendelin Boehmer, and Shimon Whiteson. My body is a cage: the role of morphology in graph-based incompatible control. In *International Conference on Learning Representations*, 2020.
- Alexander C Li, Carlos Florensa, Ignasi Clavera, and Pieter Abbeel. Sub-policy adaptation for hierarchical reinforcement learning. *International Conference on Learning Representations*, 2020.
- Minghuan Liu, Menghui Zhu, and Weinan Zhang. Goal-conditioned reinforcement learning: Problems and solutions. In *International Joint Conference on Artificial Intelligence*, 2022a.
- Minghuan Liu, Zhengbang Zhu, Yuzheng Zhuang, Weinan Zhang, Jianye Hao, Yong Yu, and Jun Wang. Plan your target and learn your skills: Transferable state-only imitation learning via decoupled policy optimization. In *International Conference on Machine Learning*, volume 162, pp. 14173–14196. PMLR, 2022b.
- Ofir Nachum, Shixiang Shane Gu, Honglak Lee, and Sergey Levine. Data-efficient hierarchical reinforcement learning. *Advances in Neural Information Processing Systems*, 31, 2018.
- Xue Bin Peng, Pieter Abbeel, Sergey Levine, and Michiel van de Panne. Deepmimic: Example-guided deep reinforcement learning of physics-based character skills. *ACM Transactions on Graphics (TOG)*, 37(4):1–14, 2018.
- Silviu Pitis, Harris Chan, Stephen Zhao, Bradly Stadie, and Jimmy Ba. Maximum entropy gain exploration for long horizon multi-goal reinforcement learning. In *International Conference on Machine Learning*, pp. 7750–7761. PMLR, 2020.
- Aravind Srinivas, Allan Jabri, Pieter Abbeel, Sergey Levine, and Chelsea Finn. Universal planning networks: Learning generalizable representations for visuomotor control. In *International Conference on Machine Learning*, pp. 4732–4741. PMLR, 2018.
- Yanchao Sun, Ruijie Zheng, Xiyao Wang, Andrew Cohen, and Furong Huang. Transfer rl across observation feature spaces via model-based regularization. In *International Conference on Learning Representations*, 2022.
- Alexander Trott, Stephan Zheng, Caiming Xiong, and Richard Socher. Keeping your distance: Solving sparse reward tasks using self-balancing shaped rewards. In *Advances in Neural Information Processing Systems*, 2019.
- Alexander Sasha Vezhnevets, Simon Osindero, Tom Schaul, Nicolas Heess, Max Jaderberg, David Silver, and Koray Kavukcuoglu. Feudal networks for hierarchical reinforcement learning. In *International Conference on Machine Learning*, pp. 3540–3549. PMLR, 2017.
- Jane X Wang, Zeb Kurth-Nelson, Dhruva Tirumala, Hubert Soyer, Joel Z Leibo, Remi Munos, Charles Blundell, Dharshan Kumaran, and Matt Botvinick. Learning to reinforcement learn. *arXiv preprint arXiv:1611.05763*, 2016.
- Tingwu Wang, Renjie Liao, Jimmy Ba, and Sanja Fidler. Nervenet: Learning structured policy with graph neural networks. In *International Conference on Learning Representations*, 2018.
- Guan Yang, Minghuan Liu, Weijun Hong, Weinan Zhang, Fei Fang, Guangjun Zeng, and Yue Lin. Perfectdou: Dominating doudizhu with perfect information distillation. In *Advances in Neural Information Processing Systems*, 2022.

Jesse Zhang, Haonan Yu, and Wei Xu. Hierarchical reinforcement learning by discovering intrinsic options. In *International Conference on Learning Representations, 2022*.

Shangdong Zhang and Shimon Whiteson. Dac: The double actor-critic architecture for learning options. In *Advances in Neural Information Processing Systems*, volume 32, 2019.

Ming Zhou, Jun Luo, Julian Vilella, Yaodong Yang, David Rusu, Jiayu Miao, Weinan Zhang, Montgomery Alban, Iman Fadakar, Zheng Chen, et al. Smarts: Scalable multi-agent reinforcement learning training school for autonomous driving. *arXiv preprint arXiv:2010.09776*, 2020.

Menghui Zhu, Minghuan Liu, Jian Shen, Zhicheng Zhang, Sheng Chen, Weinan Zhang, Deheng Ye, Yong Yu, Qiang Fu, and Wei Yang. Mapgo: Model-assisted policy optimization for goal-oriented tasks. In *International Joint Conference on Artificial Intelligence, 2021*.

Zhuangdi Zhu, Kaixiang Lin, and Jiayu Zhou. Transfer learning in deep reinforcement learning: A survey. *arXiv preprint arXiv:2009.07888*, 2020.

Appendices

A ALGORITHM OUTLINE

Algorithm 1 Planning Immediate Landmarks of Targets (PILoT)

- 1: **Source Task Input:** Empty replay buffer \mathcal{B}_s , state planner h_ψ , inverse dynamics model I_ϕ and goal planner f_ω .
 - 2: **Target Task Input:** Empty replay buffer \mathcal{B}_t , goal planner f_ω , policy π_θ .
 \triangleright *Pre-training stage* trains UDPO on **source tasks**.
 - 3: **for** $k = 0, 1, 2, \dots$ **do**
 - 4: Collect trajectories $\{(s, a, s', g^t, r, \text{done})\}$ using current policy $\pi = \mathbb{E}_{\epsilon \sim \mathcal{N}} [I_\phi(a|s, h_\psi(\epsilon; s))]$ and store in \mathcal{B}
 - 5: Sample $(s, a, s', g_t, r) \sim \mathcal{B}_s$
 - 6: **if** *learn inverse dynamics function* **then**
 - 7: **repeat**
 - 8: Update ϕ by L^I (Eq. (5))
 - 9: **until** Converged
 - 10: **end if**
 \triangleright *Distillation stage:* distill goal planner from state planner.
 - 11: Update ω by $\nabla_\omega \mathcal{L}^f$ (Eq. (9))
 - 12: **end for**
 \triangleright *Transfer stage* trains HER (PILoT) on **target tasks**.
 - 13: **for** $k = 0, 1, 2, \dots$ **do**
 - 14: Collect trajectories $\{(s, a, s', g^t, r, \text{done})\}$ using current policy π_θ
 - 15: Supplement the reward with additional bonus following Eq. (10):

$$r = r + r(s, a, \hat{g}'), \text{ where } \hat{g}' \sim f_\omega(\hat{g}'|\phi(s), g^t)$$
 - 16: Store $\{(s, a, s', g^t, r, \text{done})\}$ in \mathcal{B}_t
 - 17: Sample $\{(s, a, s', g^t, r, \text{done})\} \sim \mathcal{B}_t$
 - 18: Learn π_θ by HER
 - 19: **end for**
-

B EXPERIMENT SETTINGS

B.1 ENVIRONMENTS

We list important features of the tested environments as in Tab. 1. Note that the *Goal Reaching Distance* is rather important to decide the difficulty of the tasks, so we carefully choose them to meet the most of the current works.

Environment Name	Obs. Type	Obs. Dim	Act. Dim	Goal Dim	Goal Reaching Distance	Episode Length
Fetch-Reach	Vector	10	4	3	0.05	50
Fetch-Push	Vector	25	4	3	0.05	50
Fetch-Reach-High-Dim	Vector	10	8	3	0.05	50
Fetch-Push-High-Dim	Vector	25	8	3	0.05	50
Fetch-Reach-Image	Image	64*64*3	4	3	0.05	50
Reacher	Vector	11	3	2	0.02	50
Reacher-Image	Image	64*64*3	3	2	0.02	50
Point-Loocomotion	Vector	6	2	2	0.1	500
Ant-Loocomotion	Vector	29	8	2	0.1	100
2D-Maze	Vector	2	2	2	1.0	50
Ant-Maze	Vector	29	8	2	1.0	500

Table 1: The environments used in our experiments, where goal reaching distance denotes the range of the goal; in other words, when the agent get closer to the desired goal than the distance, the task is regarded success.

It’s worth noted that Ant robot in the common used *Ant-Maze* environment (e.g., the one used in Pitis et al. (2020); Eysenbach et al. (2022)) is different the one in *Ant-Locomotion* (e.g., the one used in Zhu et al. (2021)), like the *gear* and *ctrlrange* attributes. Thus, in order to test the transferring ability, we synchronize the Ant robot in these two tasks and re-run all baseline methods on these tasks.

B.2 ACTION DYNAMICS SETTING FOR HIGH-DIM-ACT CHALLENGE

For transferring experiments on High-Dim-Act challenge, we take an 80% of the original gravity with a designed complicated dynamics for the transferring experiment (different both action space and dynamics). Particularly, given the original action space dimension m and dynamics $s' = f_s(a)$ on state s , the new action dimension and dynamics become $n = 2m$ and $s' = f_s(h(a))$, where h is constructed as:

$$h = -\exp(a[0 : n/2] + 1) + \exp(a[n/2 : -1])/1.5$$

here $a[i : j]$ selects the i -th to $(j - 1)$ -th elements from the action vector a . In other words, we transfer to a different gravity setting while doubling the action space and construct a more complicated action dynamics for agent to learn.

B.3 IMPLEMENTATION DETAILS

The implementation of PILoT and HER are based on a open-source Pytorch code framework¹. As for compared baselines, we take their official implementation, use its default hyperparameters and try our best to tune important ones:

- MEGA (Pitis et al., 2020): <https://github.com/spitis/mrl>
- HIGL (Kim et al., 2021): <https://github.com/junsu-kim97/HIGL>
- Contrastive RL (Eysenbach et al., 2022): https://github.com/google-research/google-research/tree/master/contrastive_rl

For resolving image-based tasks, we learn an encoder that is shared between the policy and the critic. In particular, we use the same encoder structure for HER, MEGA and HIGL. The encoder has four convolution layers with the same 3×3 kernel size and 32 output channel. The stride of the first layer is 2 and the stride of the other layers is 1, as shown in Fig. 7. We adopt ReLU as the activation function in all the layers. After convolution, we have a fully connected layer with 50 hidden units and a layer-norm layer to get the output of the encoder. When training, only the gradients from Q network are used to update the encoder. For contrastive RL, we take their default structures for image-based tasks.

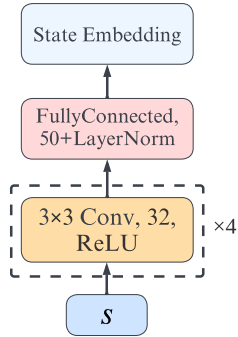


Figure 7: The encoder network architecture.

B.4 IMPORTANT HYPERPARAMETERS

We list the key hyperparameters of the best performance of HER in Tab. 2 and UDPO in Tab. 3 on each source task. For each task, we first tune HER to achieve the best performance, based on which we further slightly adjust UDPO’s additional hyperparameters.

For HER, we tune *Replay buffer size* $\in \{1e5, 1e6\}$, *Batch size* $\in \{128, 2048, 4096\}$, *Policy π learning rate* $\in \{3e - 4, 1e - 3\}$.

For UDPO, we only tune two hyperparameters, *State planner coefficient* $\lambda \in \{1e - 3, 5e - 3, 1e - 2, 5e - 2, 1e - 1\}$, *Inverse dynamics I learning interval* $\Delta \in \{200, 500, 1500, 2000\}$. As further shown in Section C.2, the choice slightly affects the success rate but can impose considerable influence on the accuracy of the state planner. The larger λ will lead stronger constraint on the accuracy

¹<https://github.com/Ericonaldo/ILSwiss>

of the state planner, but can hurt the exploration. On the other hand, Δ controls the training stability, and a larger Δ assumes that the local inverse dynamics does not change for a longer time. Therefore, in principle, for those tasks that exploration is much more difficult, we tend to choose a small λ ; for those tasks that the algorithm can learn fast so that the local inverse dynamics changes drastically, we should have a small Δ . In default, we choose $\lambda = 1e - 2$ and $\Delta = 1500$.

We also list the hyperparameters of HER (PILoT) in Tab. 4 on each target task, which is the same as the baseline HER algorithm (except the additional *Transferring bonus rate*.) In default, we set all *Transferring bonus rate* to be 1.0, and find that it can reach a desired performance. In Section C.2, we also include the ablation of the choice of this hyperparameter.

Table 2: Hyperparameters of HER on the source tasks.

Environments	Fetch-Reach	Fetch-Push	Reacher	2D Maze	Point-Loconotion
Optimizer	Adam Optimizer				
Discount factor γ	0.99				
Replay buffer size	1e5	1e6	1e6	1e5	1e6
Batch size	128	2048	2048	128	2048
Number of VecEnvs	1	8	4	1	4
Q learning rate	3e-4				
Policy π learning rate	3e-4	1e-3		3e-4	

Table 3: Hyperparameters of UDPO on the source tasks.

Environments	Fetch-Reach	Fetch-Push	Reacher	2D Maze	Point-Loconotion
Optimizer	Adam Optimizer				
Discount factor γ	0.99				
Replay buffer size	1e5	1e6	1e6	1e5	1e6
Batch size	128	2048	2048	128	2048
Number of VecEnvs	1	8	4	1	4
State planner coefficient λ	1e-2			1e-1	5e-3
Q learning rate	3e-4				
Policy π learning rate	3e-4	1e-3		3e-4	
Inverse dynamics I learning rate	1e-4				
Inverse dynamics I learning interval Δ (epochs)	200			1500	

Table 4: Hyperparameters of HER / HER (PILoT) on the target tasks.

Environments	Fetch-Reach-High-Dim	Fetch-Push-High-Dim	Fetch-Reach-Image	Reacher-Image	Ant-Loconotion
Optimizer	Adam Optimizer				
Discount factor γ	0.99				
Replay buffer size	1e5	1e6			
Batch size	128	2048			4096
Number of VecEnvs	1	8	1	4	4
Q learning rate	3e-4				
Policy π learning rate	3e-4	1e-3	3e-4	1e-3	1e-3
Transferring bonus rate	-	-	1.0		

C MORE EXPERIMENTAL RESULTS

C.1 DOES UDPO REACH WHERE IT PREDICTS?

In the universal decoupled policy structure, the state planner is decoupled and trained for predicting the future plans that the agent is required to reach. Therefore, it is critical to understand the plans given by the planner and make sure it is accurate enough that the agent can reach where it plans to go, for distilling and transferring. To this end, we analyze the distance of the reaching states and the predicted consecutive states and draw the mean square error (MSE) along the RL leaning procedure in Fig. 8. To our delight, as the training goes, the gap between the planned states and the achieved states is becoming smaller, indicating the accuracy of the state plan.

Additionally, we also visualize the imagined rollout by state planner on the source tasks, which is generated by consecutively take a predicted states as a new input. We compare it with the real rollout in Fig. 9, showing the state planner can conduct reasonable multi-step plan.

On the target tasks, we visualize the subgoals proposed by the distilled goal planner and the real rollout that was achieved during the interaction in Fig. 10, showing the effective and explainable guidance from the goal planner.

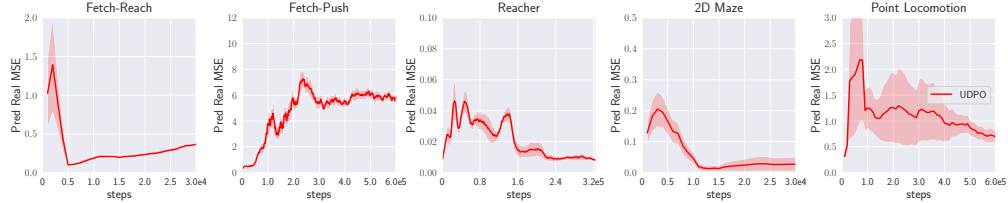


Figure 8: Curves of the MSE between one-step prediction of the state planner and the real state achieved in the source environments.

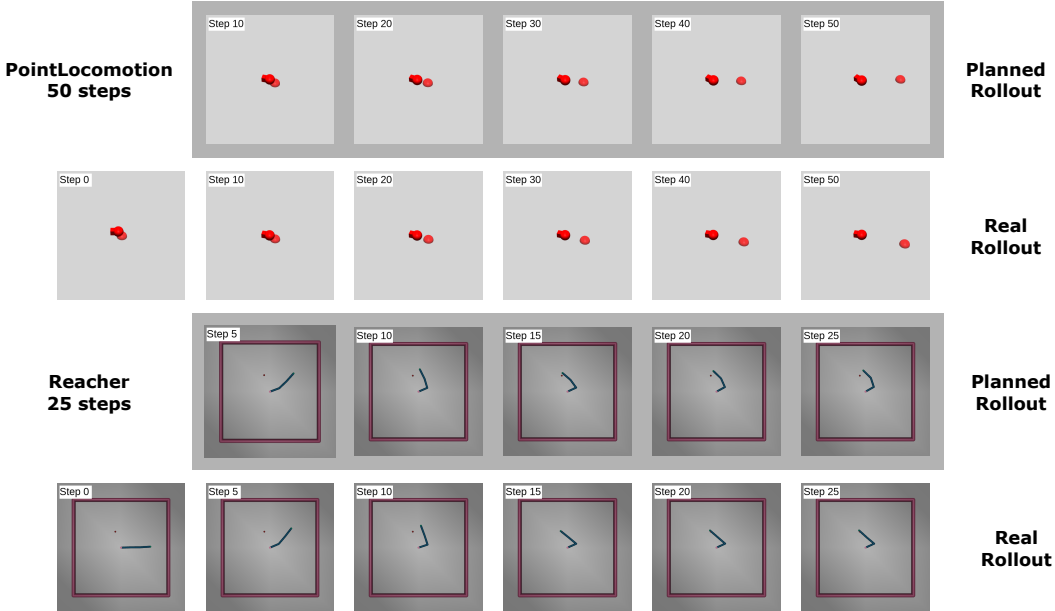


Figure 9: Imagined rollout by state planner and the real rollout that was achieved during the interaction in two source tasks, showing the reasonable multi-step plan of the state planner. For Fetch-R reach and Fetch-Push environments, we cannot render the planned rollout since the simulator internal states can not be recovered from agent observations.

C.2 ABLATION STUDY

In this section, we aim to investigate the robustness and the key components of our proposed PILoT framework. Specifically, we first analyse the two critical hyperparameters, *i.e.*, the inverse dynamic train frequency Δ and the regularization coefficient λ on training UDPO in the pre-training stage; then, we provide additional ablation analysis on bonus ratio β in the transferring stage.

Pre-training ablation on the inverse dynamic train frequency Δ . We first conduct ablation studies on the inverse dynamic train frequency Δ . In particular, this hyperparameter determines how often we train the low-level inverse dynamics and how long we regard the inverse dynamics is static when we train the high-level state planner. It is intuitive that a larger Δ is assuming that the local inverse dynamics does not change for a longer time; on the contrary, a small Δ should be used when the the local inverse dynamics changes drastically. In our experiments, we find that Δ affects

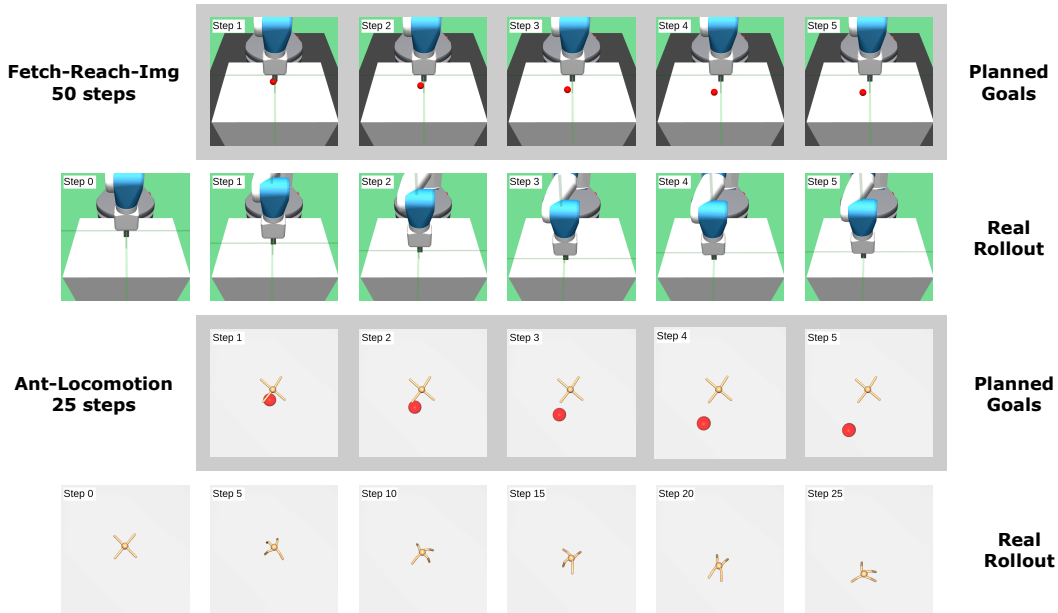


Figure 10: Subgoals proposed by the distilled goal planner and the real rollout that was achieved during the interaction in two target tasks, showing the effective and explainable guidance from the goal planner. For Ant-Loocomotion environment, the goal planner is distilled from Point-Loocomotion environment, in which the point agent has faster moving speed than the ant. Nevertheless, the resultant trajectory in Ant-Loocomotion can still match the planned goals roughly.

the training stability, as it embeds some prior about the policy training in certain tasks. As is shown in Fig. 11, *Fetch-Push* requires smaller Δ than *Point-Loocomotion*, since *Fetch-Push* is more simple, and the policy training is much faster than the policy training in the *Point-Loocomotion*.

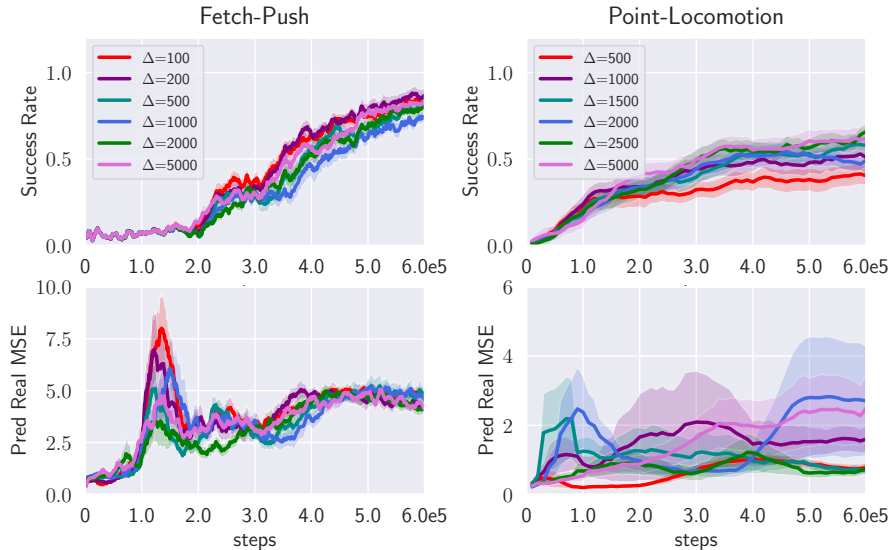


Figure 11: Ablation study on inverse dynamic train frequency Δ with 5 seeds, given the other parameters the same in Section 6.2.

Pre-training ablation on the regularization coefficient λ . The regularization coefficient λ is another critical hyperparameter in UDPO training. The choice of λ balances the policy gradient term and the constraint term in state planning updates. Particularly, larger λ puts more weight on the

supervised penalty objective, which reduces the planning of infeasible next states. However this can hurt the exploration ability offered by policy gradient objective. The results in Fig. 12 supports the intuition. In both environments, the models trained with $\lambda = 0.1$ performs best in reaching where they plan, but can not finish the goal-reaching task well. On the other hand, a extreme small λ results in a quite large gap between reached states and planned states. Such gap can make the subsequent transferring impossible. Therefore, the recipe is to find the medium λ which achieves competitive success rate while keeping the value of prediction real MSE from explosion.

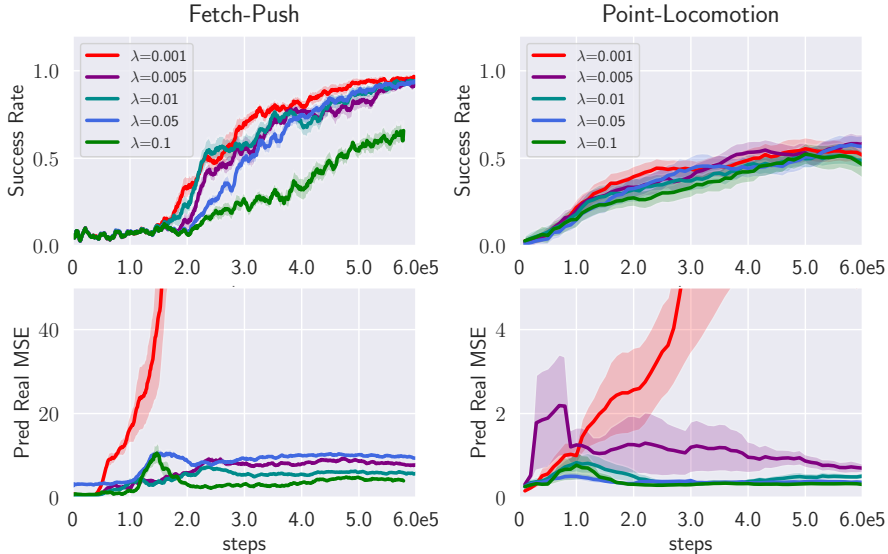


Figure 12: Ablation study on state planner coefficient λ with 5 seeds, given the other parameters the same in Section 6.2.

Transferring ablation on the bonus ratio β . In the transferring stage, bonus ratio β balances the similarity reward from distilled planner and the sparse reward from the environment. We observe from Fig. 13 that 1.0 is an appropriate choice for at least tasks tested in this paper. When β is smaller (e.g., 0.1, 0.2, 0.5), the success rate converges more slowly, and the final performance is also worse. This indicates that small β can not provide strong enough signals for the policy to follow planned landmarks, leading to a decreased transfer efficiency. On the other hand, when a much larger β (e.g., 2.0, 5.0) is adopted, the performance becomes even worse than insufficient guidance from small β . Also, in Fetch-Reach-Image environment, the training curves are quite unstable. Although the planned landmarks are useful in overcoming the sparse reward issue, they can not completely replace the final sparse reward. As Fig. 8 shows, even in the source environments, there exist small but not negligible errors between planned states and achieved states. Using large β can let the policy misled by the goal planner and overfitted to those errors.

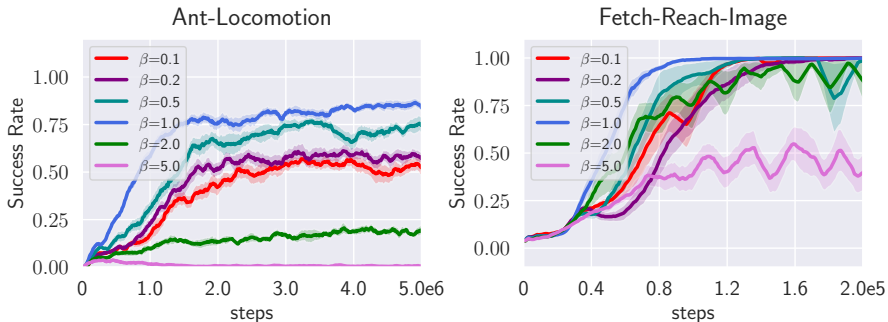


Figure 13: Ablation study on bonus ratio β with 5 seeds, given the other parameters the same in Section 6.2.

C.3 MORE ZERO-SHOT TRANSFER VISUALIZATION

In this section we illustrate more zero-shot transfer cases including success cases and failure cases. In fact, the failures should be attributed to the inaccuracy of the controller (policy) since the goal planner always gives the right way to success. If we can train a more accurate local controller, the performance of success rate can no doubt be further improved.

C.3.1 SUCCESS CASES

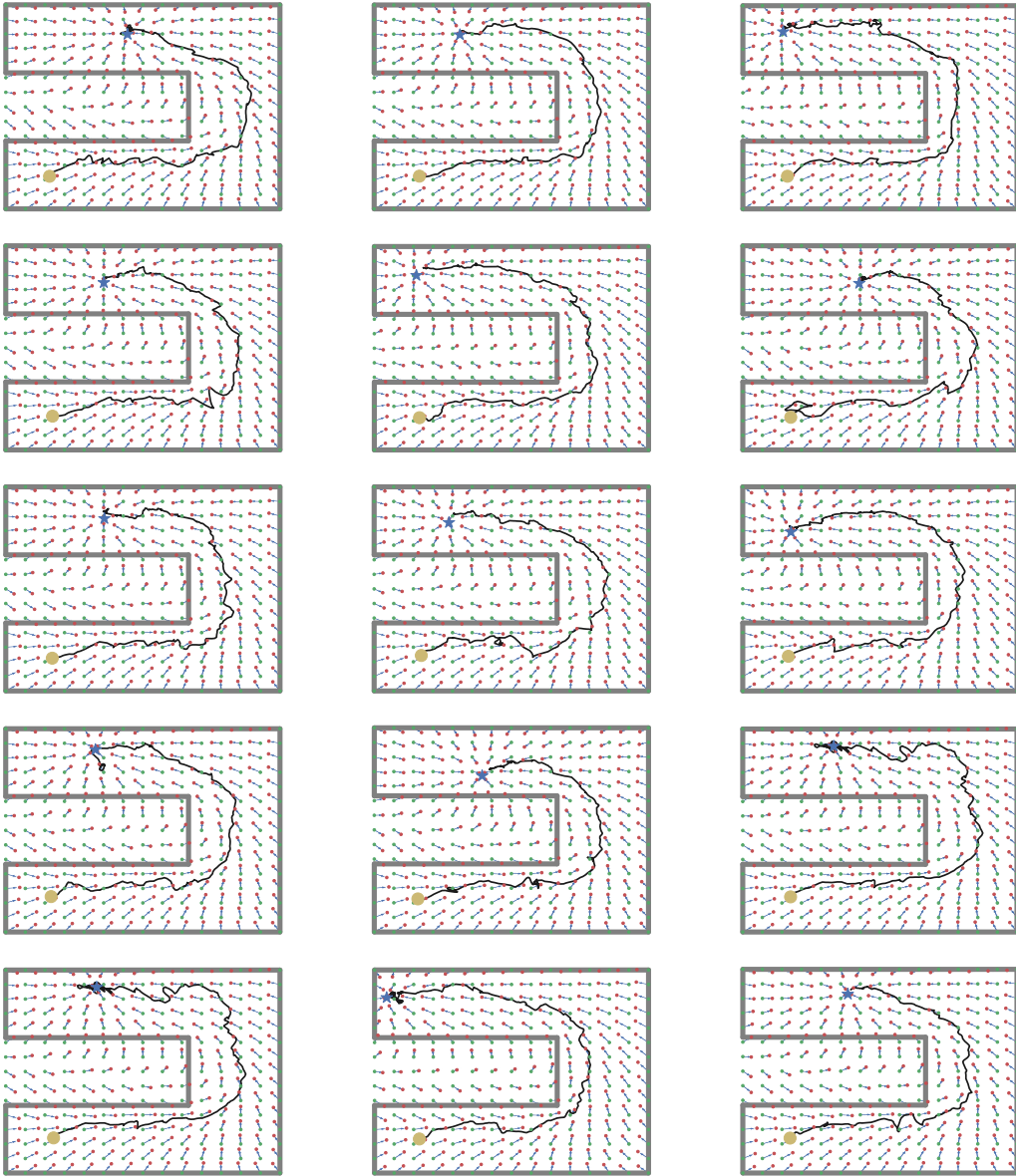


Figure 14: Success cases of zero-shot transfer on Ant-Maze.

C.3.2 FAILURE CASES

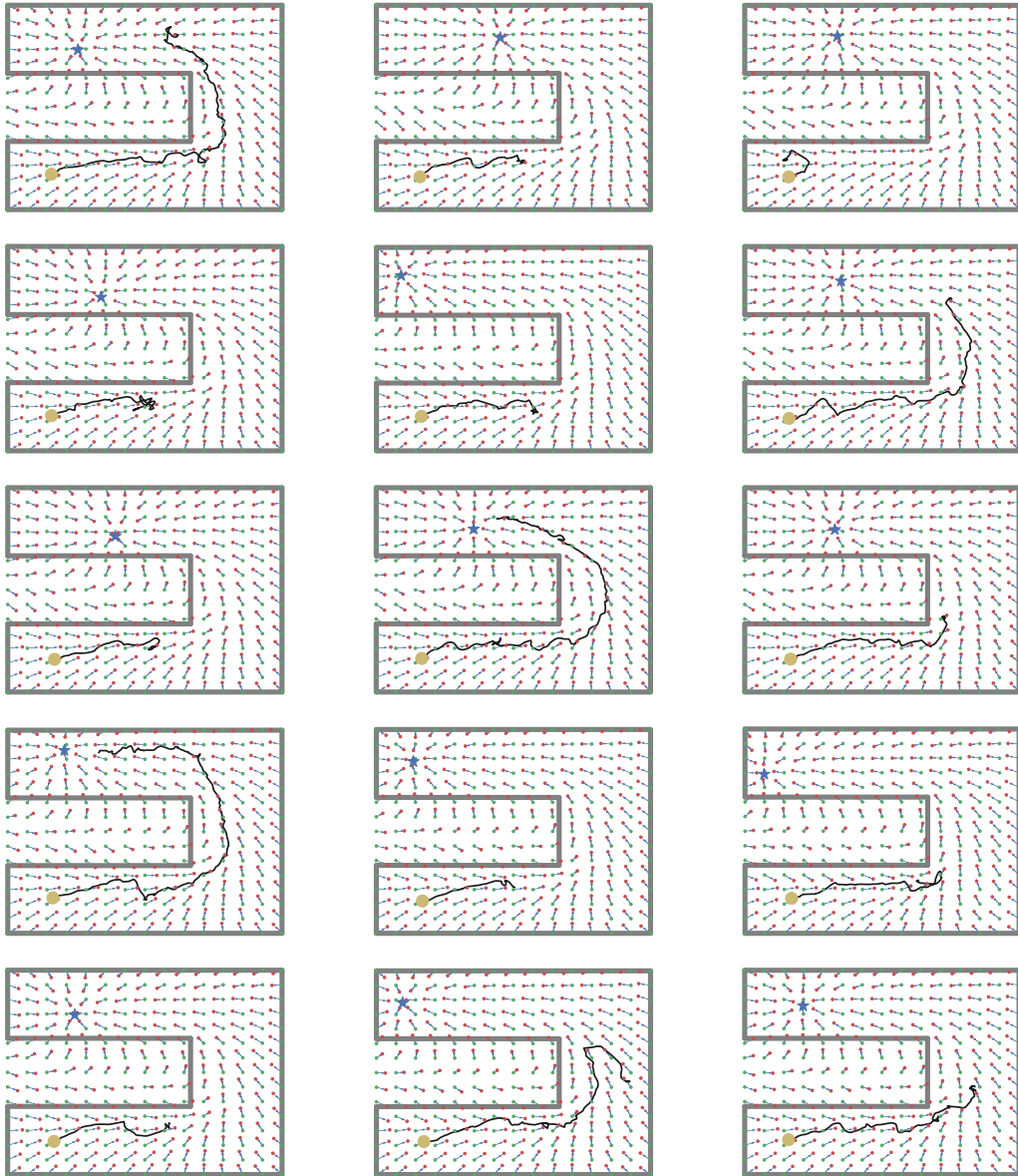


Figure 15: Failure cases of zero-shot transfer on Ant-Maze.